4th International Conference on Science, Technology and Management
India International Centre, New Delhi (ICSTM-16)
15th May 2016, www.conferenceworld.in ISBN: 978-81-932074-8-2

SYNTHESIS AND CHARACTERIZATION OF $BACE_{0.85}Y_{0.15}O_3$ SOLID OXIDE FUEL CELL ELECTROLYTE BY CITRATE EDTA COMPLEXING SOL-GEL PROCESS

Jampana Madhuri Sailaja[1], V.Veeraiah[2]

[1,2] *Department of Physics, Andhra University, Vishakhapatnam, Andhra Pradesh, (India)*

ABSTRACT

This paper reports on the effect of Yttrium doping on $BaCeO_3$ electrolyte prepared using the citrate-EDTA complexing sol-gel process at temperature T=1000°C. The phase formation and evolution with the temperature has been studied by X-ray diffraction (XRD), thermal analysis (TG-DTA).

The morphology of the sintered powder at T=1300°C are examined by

- *SEM - Scanning Electron Microscopy*
- *FTIR - Fourier transforms infrared spectrometer*
- *FTRS-Raman measurements*

The crystallite size of the ceramic powders calculated from Scherrer equation is 32nm and the diffraction peak shifted to higher angles. Microstructure of the sintered powder revealed that the average grain size is in the range of 2-3μm. Dense ceramic materials were obtained at 1300°C and the relative density is 89% of the theoretical density. FTIR and Raman measurements reveal the complete single phase formation of the orthorhombic perovskite structure. The ionic conductivity of the pellet is investigated from room temperature to 400°C and is found to be $7.7x10^{-4}$S/cm (400°C). The conductivity increased as temperature increases and the activation energies is 0.56eV and hence this composition is worth being electrolyte.

Keywords: Proton conducting electrolyte, BaCe $_{0.85}Y_{0.15}O_3$, Sol-Gel synthesis, Fuel Cells, Raman spectra.

I. INTRODUCTION

During the past few decades, Hydrogen has been identified as fuel in the fields of electric power generation and transportation. It is arising as future renewable energy option due to increasing environment pollution aspects [1-3].The aim is to synthesis a dense ceramic conductor with good chemical stability at high temperatures. Recently SOFCs based on proton conducting electrolytes (SOFC-H^+) have attracted much attention due to their relatively low temperature operation (400-800°C) that aids in better sealing and interconnection of the materials, lowering the thermal expansion mismatch between the cell components [4]. But operating at such high temperatures probe practical problems like excessive costs, material degradation, prolonged start up and shut off

periods [5,6].To solve these issues many researchers have developed various new electrolyte materials to reduce the sintering and operating temperatures.

Perovskite–type oxides such as $BaCeO_3$, $BaZrO_3$, $SrZrO_3$ and $SrCeO_3$ are known to protonic conductors among which $BaCeO_3$ has highest protonic conductivity among them [7, 8].Generally, the ceramic electrolytes are synthesized by means of solid-state reaction (SSR) method which involves extensive ball-milling, repetitive grinding and high-temperature treatment (T=1,400°C).As a result, some impurities may instigate in the heat treatment process which provokes into material degradation. To overcome the SSR complications, wet chemical methods (WCMs) like sol–gel, hydrothermal, co-precipitation, [9-11] is espoused to obtain the desired perovskite compound. With the help of these methods fine powder morphology with less contamination can be procured. Sol-gel and Pechini method utilizes the features of both citric acid &ethylenediaminetetra acetic acid (EDTA) to form polybasic acid chelated with various metal cations [12-13]. Iwahara et al. [14] studied the effect of ionic radii of dopants on mixed ionic conduction ($H^+ + O^{2-}$) in $BaCe_{0.9}M_{0.1}O_{3-\delta}$ (M=Yb, Y, Dy, Gd, Sm, Nd) and found that, as the ionic radius of the dopant increases, the spacing along the a-axis of these materials becomes longer in approving of the increased combination of oxide ion to the total conduction. Therefore Y is introduced in the B site to partially replace Ce ions in the present work and study the dependence of ionic conductivity on lattice volume [16] of the perovskite.

II. EXPERIMENTAL

Powder preparation

The citrate-EDTA complexing sol-gel procedure is used for preparing $BaCe_{0.85}Y_{0.15}O_3$ oxide. The starting materials for this process are commercial $Ba(NO_3)_2$, $ZrO(NO_3)_2.2H_2O$, $Ce(NO_3)_36H_2O$ (High Media, 99.5%). Both citric acid and EDTA are added to the precursor solution as chelating agents. The citric acid molar ratio and EDTA to the total metal cations content was set at 1:2:1. The pH value of the solution was adjusted to be around 6 using NH_4OH. The mixed solutions were heated under stirring until obtaining viscous gels at T=100°C. Additional heating at T=250°C evaporates residual water & organics, later these gels were transformed into black powders. The synthesized powder is then calcined at T=1000°C for 12h with a heating rate of 5°C/min. To obtain dense sample, the calcined powder is uniaxially pressed into cylindrical pellet under 5 ton pressures for 5min and then sintered in an air atmosphere. Sintering was carried out at T=1300°C for 5h at a heating rate of 5°C /min.

III. CHARACTERIZATION

Thermo gravimetric analysis (TGA) are performed to the dried powder (T= 250°*C)* by a TA instrument model SDT Q 600. The phase identification of the sintered oxides is performed with a powder Diffractometer (PANalytical X-pert Pro) with Ni filtered Cu Ka radiation and the diffraction angle from 10° to 90° with a step of 0.01°/min. Morphologies of the sintered pellet is examined using scanning electron microscope JEOL model JSM-6610 LV in conjunction with an energy dispersion spectrometer (EDS) to find out the percentage of elements present in the sample. A FTIR spectrometer (SHIMADZU IR Prestige-21, Singapore) is used to record the FTIR spectra of $BaCe_{0.85}Y_{0.15}O_3$ powder in the range of 4,000-400$cm^{-1}$and in turn investigate the complex

structure, carbonates and oxides formation. The theoretical density of the powder is calculated with the obtained XRD. FTRS-Fourier transforms Raman spectroscopy (BTC111-RAMAN-785) studies were conducted to study the vibrational modes of the samples in the range 0-1000cm^{-1}.LCR measurements from room temperature to 400°C were performed with Wayneker P6500 model in the frequency range from 20Hz to 1 MHz.

The crystallite sizes of the powder are calculated using Scherrer's formula Eq. 1:

$$D_p = \frac{0.94\lambda}{\beta \cos\theta} \quad (1)$$

Where

- D_p= Average crystallite size
- B =FWHM
- θ =Bragg angle
- λ = X-ray wavelength.

The bulk density of the sintered pellet is determined using Archimedes displacement method.

IV. RESULTS AND DISCUSSION

Thermogravimetry / Differential Thermal Analysis

To investigate the reaction of the perovskite phase structure formation, simultaneous TG-DTA curves of the sample conducted from room temperature to 1200°C are presented in Fig.1.In terms of thermal stability nitrates are unstable than carbonate and hence are easy to decompose.

From Fig.1 it can be seen that three regions are obtained in TG-DTA of the powder. The gradual weight loss is 18% up to 200°C and is due to absorption of water molecules. The additional weight loss along with exothermal peaks in DTA reveals that the decomposition of gel takes place in two steps. The weight loss from 200°C to 500°C is found to be 21% accompanied with small exothermic peak at 418°C is due to combustion of the metal nitrates. The drastic weight loss occurred from 500-630°C (25%) and the exothermic peak at T=573°C is due to co-oxidation. A very small weight loss is observed at T >1000°C which is due to barium carbonate thermal decomposition, also detected in XRD. TG curve displays a drastic weight loss starting at around 500°C with a corresponding exothermic effect, which is related decomposition of $BaCO_3$ and the formation of powder with the release of CO_2 [18-19]. This is consistent with the XRD results from the Fig.2 that $BaCe_{0.85}Y_{0.15}O_3$ phase only forms upon calcining at 1000°C and above. There is no apparent weight change is depicted when the temperature is higher than 1100°C, indicating complete phase formation of the compound.

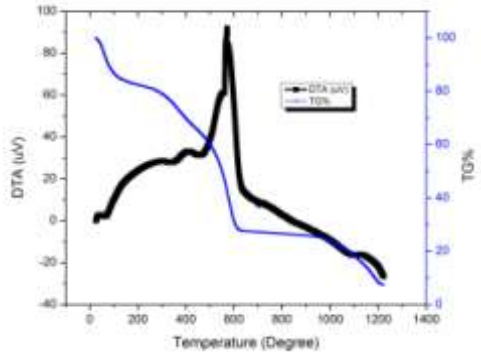

Fig. 1 TG-DTA curves of BaCe $_{0.85}Y_{0.15}O_3$powder preheated at 250^{0}C for 24h.

V. X-ray DIFFRACTION (XRD) ANALYSIS

The phase compositions of BaCe $_{0.85}Y_{0.15}O_3$powder has been identified by X-ray diffraction (XRD) analysis. The experimental diffraction pattern is collected at room temperature by step scanning at 0.01°/min over the range $10^{\circ} \leq 2\theta \leq 90^{\circ}$. As shown in Fig.2 sintered oxides are predominantly the perovskite dominant structure with five major diffraction signals (002), (022), (213), (611), and (422) planes (JCPDS Card no. 22-0074). The XRD patterns of powders calcined at T=1000°C for 12 h showed a single orthorhombic phase Fig.2 with pnma space group according to Knight et al. [18-22]. The cell parameters were determined by least-square refinements and the calculated lattice parameters are found to be a=8.6998, b=6.2587, c=6.2339 and cell volume is 339.4323(Å) ^{3} with a relative density of 89%. It was reported that phase formation in $BaCeO_3$ obtained from solid state synthesis requires calcinations at 1100°C or 1200°C for 10h or more .Such high temperatures can result in grain growth which causes decrease in surface area of the powder and sintered density. In the present method of preparation, 1000°C is sufficient to form a single phase material by adjusting the pH to 6 which liberates more protons from citric acid that helps to chelate Ba ions and enhance phase formation.

Close examination of the XRD data projects that as Yttrium is doped in the B sites the diffraction peak shifted to higher angles and increase of the lattice parameters along with lattice volume is observed than $BaCeO_3$ (experimental value 339.376 reported elsewhere), which suggests a plane distance reduction (according to Bragg's law).This can be well explained by the fact that Y^{3+}has a smaller ionic radius than Ce^{4+} [17].

The crystallite size is examined from XRD peaks based on the Scherrer equation, and the results showed that the particle size of the synthesized sample is around 32 nm.

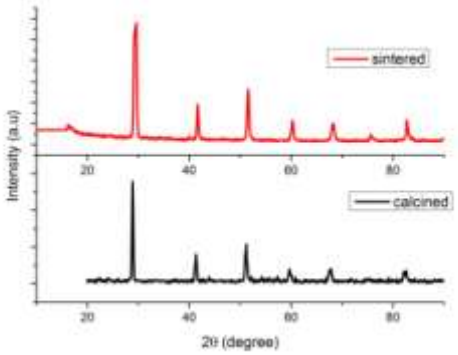

Fig. 2 XRD patterns of calcined (1000°C) and sintered BaCe $_{0.85}Y_{0.15}O_3$ (1300°C) oxides.

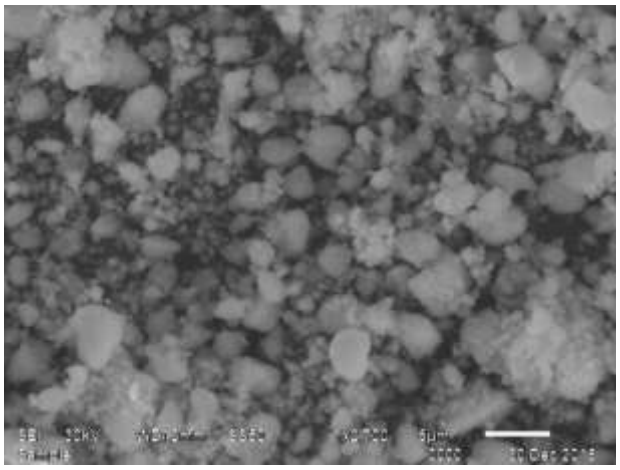

Fig.3. SEM morphologies of sintered (1300^{0}C/5h) $BaCe_{0.85}Y_{0.15}O_3$ oxides.

VI. MICROSTRUCTURE

The surface morphology of the sintered powder is shown in the Fig.3 depicts a heterogeneous distribution of grains with an average size in the range of 2-3μm. This is consistent with the fact that the grain size decreases as the ionic radius of the dopant decreases. Dense ceramic materials were obtained at T=1300°Cand the relative density is 81% of the theoretical density.

VII. FTIR - FOURIER TRANSFORMS INFRARED SPECTROSCOPY

FTIR spectrum of the sintered powder is shown in Fig.4. FTIR analysis is used to explain in further detail the formation of the carbonate species during heat treatment. The high intense peak near 860cm^{-1}may be due to the =C-H bend. The peak localized in the range of 1436cm^{-1} is attributed to the C-H bend and which may be due to the complex formed from a chealation process of chelating agents, carboxyl acids and metal ions [19-21].

FTRS- Fourier transforms Raman spectroscopy

Raman spectra recorded at room temperature is shown in the Fig 5. Raman Spectroscopy can not only be considered as an important tool in measuring the degree of cation ordering but also used to study dynamic changes in a structure. The small peak in the range 116 cm^{-1} might be assigned to the stretching mode of the carbonate ion around the strontium ion. The Raman band around 352cm^{-1} is refers to O-B-O bending in ABO_3 perovskites. A small band near 500cm^{-1} was attributed to torsional mode of the B-O bond of the B sites and between 450-550cm^{-1} is CeO_2 like peak[22,23].The small peak near 700cm^{-1} can be attributed to the symmetric metal-oxygen stretching vibrations of the BO6 octahedra [24,25].Increase in ionic radius of the doped atoms lead to a more distortion from orthorombhic strucrure with a corresponding decrease in raman active vibration bands which results in a more symmetric structure confirming the phase structure remaning the same with the introduction of yttrium into the structure.

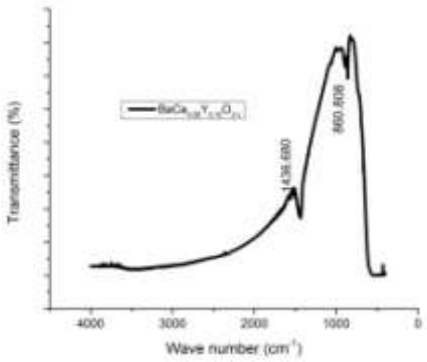

Fig. 4. FTIR spectra of sintered (1300^{0}C/5h) BaCe $_{0.85}Y_{0.15}O_3$oxides.

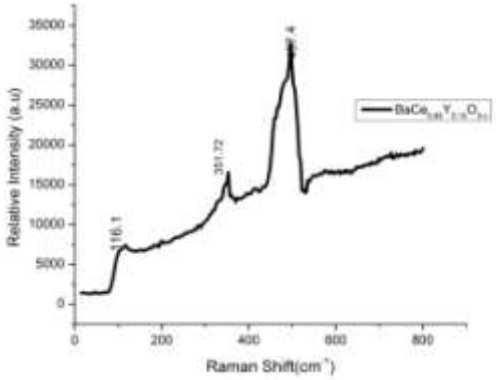

Fig. 5. Raman spectra of sintered (1300^{0}C/5h) BaCe $_{0.85}Y_{0.15}O_3$oxides.

VIII. IMPEDANCE ANALYSIS

The impedance spectra measured in air from 200˚C to 400°C in dry air is shown in the Fig.6.Theoritically the spectra comprises of three arcs at high, medium and low frequencies, corresponding to the response of bulk, grain boundary and the electrode respectively [26, 27] in the Nyquist plots (Z' vs. Z'').In the Nyquist plots of the present work, the high frequency semi circle related to bulk response could not be seen due to the instrumental limitations of the experimental range. Therefore, the bulk response is assigned to the high frequency intercept of the medium arc with the real axis.

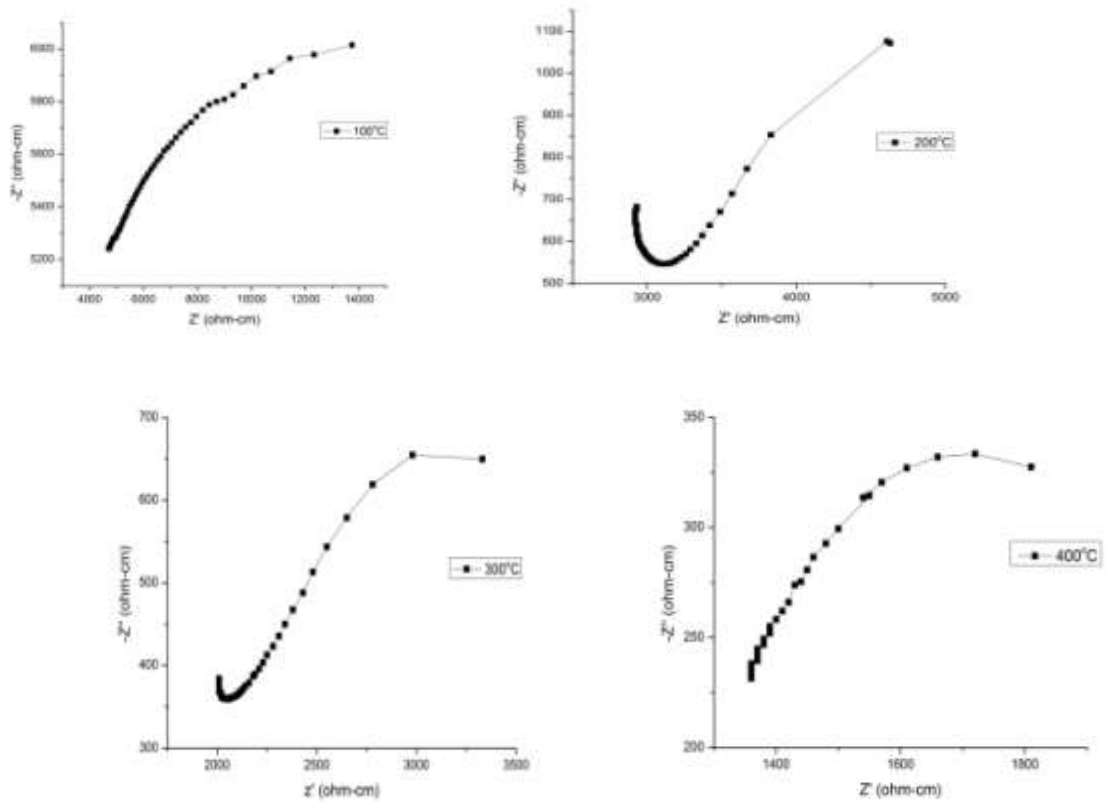

Fig 6 Nyquist plots at various temperature in air for sintered (1300°C) $BaCe_{0.85}Y_{0.15}O_3$oxides.

The Arrhenius plots were obtained from the conductivity data using the Arrhenius equation given in Eq. 2.

$$\sigma_{ac} = \sigma_o \, exp\left(\frac{-E_a}{K_b T}\right) \quad (2)$$

Where

- σ_o is the pre-exponential factor
- Ea is the activation energy
- k_B Boltzmann constant
- T is the absolute temperature respectively.

In air atmosphere, the Arrhenius plot of the sample followed a linear trend from 200°C to 400°C as shown in the Fig. 7. Here, the conductivity has a lower value with slightly higher activation energy in air when compared to wet atmosphere as there is no presence of water for proton conduction mechanism to take place. The conductivity valuesof $BaCe_{0.85}Y_{0.15}O_3$ is found to be $7.4x10^{-4}$S/cm and the conductivity increased with increase in temperature. The activation energy (0.56eV) is determined from the slope of the plot Logσ vs. 1000/T are which is comparable with that of the reported value available in literature [15,30].

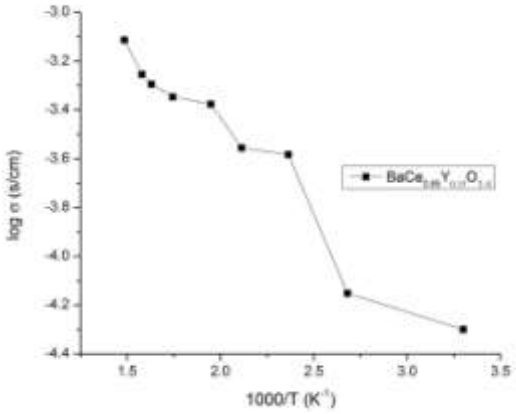

Fig. 7. Arrhenius plot of conductivity in air for samples sintered at 1300^{0}C/5h BaCe $_{0.85}$Y$_{0.15}$O$_3$oxides.

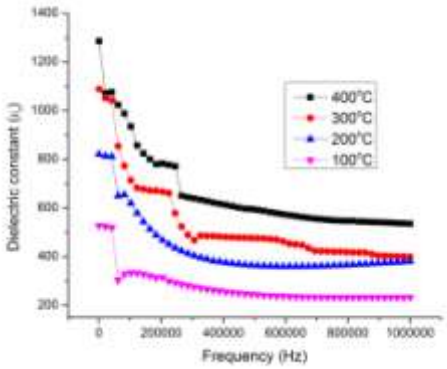

Fig 8.Dielectric constant vs frequency plot of sintered (1300^{0}C/5h) BaCe $_{0.85}$Y$_{0.15}$O$_3$ oxides.

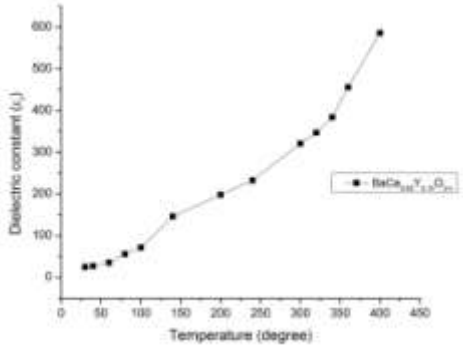

Fig. 9. Variation of Dielectric constant with Temperature of sintered (1300^{0}C/5h) BaCe $_{0.85}$Y$_{0.15}$O$_3$ oxide.

The variation of Dielectric constant with temperature (50°-400°C) and frequency (20Hz to 1MHz) is studied. From the frequency dependent plot Fig.8 it is evident that the value of ε_r decreases sharply as the frequency increases .The higher values of dielectric constant at low frequencies can be affliated to space charge polarization (power frequencies) which occurs due to pile up of charges at the interfaces between the sample and the electrode. In low frequency regions the diploes will get sufficient time to orient themselves completely along the field direction when the sample is subjected to an alternating field resulting in larger values of ε_r of the samples. As the frequency increases further, the dipoles in the samples cannot reorient themselves in pace to the to the applied electric field but lags behind, resulting in the decrease in ε_r of the samples up to 10^6 Hz.

From the plot of dielectric constant versus temperature Fig.9, it was proved that as temperature increased the dielectric constant also increased. This can be explained as follows. In space charge polarization, the increase in temperature facilitates the diffusion of ions. Additionally, thermal energy may also help in overcoming the

activation barrier for the orientation of polar molecules in the direction of the field which increases the value of ε_r.

The conductivity and activation energy values determined in the present work with reference to other works are listed in the Table 1.

Table 1. Conductivity and activation energies of various compositions.

Composition	Sintering Temperature	Conductivity (S/cm)	Activation energy(eV)	Reference
$BaCeO_3$	1300°C/2hrs	$5.13x10^{-5}$ (500°C)	0.70	[27]
$Ba_{0.9}Sr_{0.1}CeO_3$	1300°C/2hrs	$2.55x10^{-4}$ (500°C)	0.61	[27]
$BaCe_{0.95}Y_{0.05}O_{3-\delta}$	1550°C/10hrs	$1.9x10^{-3}$ (800°)C		[15]
$BaCe_{0.8}Zr_{0.1}Nb_{0.1}O_{3-\delta}$	1500°C/24hrs	$5.6x10^{-4}$ (500°C) wet H_2		[28]
$BaZr_{0.8}Y_{0.2}O_{3-\delta}$	1400°/10hrs	$1.17x10^{-6}$(400°)C		[30]
$BaCe_{0.85}Y_{0.15}O_{3-\delta}$	1300°/5hrs	$7.4x10^{-4}$ (400°)C	0.6	This work

IX. CONCLUSION

$BaCe_{0.85}Y_{0.15}O_{3-\delta}$ has been successfully synthesized using the citrate-EDTA complexing sol-gel process at low temperature as low as T=1000°C.The sample showed single phase orthorhombic structure with pmna space group and is consistent with the standard JCPDF data. The crystallite size of the ceramic powders is calculated from Scherrer equation and is found to be 32nm and the diffraction peaks shifted to higher angles. Microstructure of the sintered powder revealed that the average grain size is in the range of 2-3μm. Dense ceramic materials were obtained at 1300°C and the relative density is 89% of the theoretical density. FTIR and Raman measurements reveal the complete of the orthorhombic perovskite structure single phase formation. The ionic conductivities of the pellet are investigated from room temperature to 400°C and is found to be $7.4x10^{-4}$ S/cm.The conductivity increased as temperature increases and the activation energies is 0.56eV .From the results above it is proved that this method of preparation yields good electrolyte which exhibited enhanced conductivity value at low sintering temperature with increased density. Further increase in sintering temperature may increase the density but there is a chance of evaporation of Ba at high temperatures. Further research on using of sintering aid to obtain dense samples without rise in sintering temperature along with trivalent dopants is under process.

X. ACKNOWLEDGEMENTS

The authors wish to thank the Coordinator DST-Purse programme, Advanced Analytical laboratory, Andhra University for providing XRD, SEM, FTIR and LCR measurements used in this work.

REFERENCES

[1] EP. Murray,T .Tsai, S.A .Barnett, A direct-methane fuel cell with a ceria-based anode, Nature 400 (1999) 649-51.

[2] S.H Chan, Hohk, Y.Tian, Multi-level modeling of sofc-gas turbine hybrid system, Int J.Hydrogen energy. 28 (2003) 899-900.

[3] S.M Haile, Fuel cell materials and components, Acta Mater. 51 (2003) 5981-6000.

[4] Siriwan Chokka SutinKuharuangrong, Effect of Sr and Y on microstructure and electrical conductivity of BaCeO3, Songklanakarin J.Sci.Technol. 35(5) (2013) 557-561.

[5] K .Ie, R.Q Yanb, X.Q Liua, Stable $BaCe_{0.7}Ti_{0.1}Y_{0.2}O_{3-\delta}$ Proton conducting for solid oxide fuel cells, J Alloys Compd. 479 (2009) 40-2.

[6] I.M Hung, H.W Peng, S.L Zheng, C.P Lin, J.S Wu, Phase stability and conductivity of $Ba_{1\ y}Sr_yCe_{1-x}Y_xO_{3-d}$ solid oxide fuel cell electrolyte, J Power Sources. 193 (2009) 155-9.

[7] T.Takahashi, H.Iwahara, Proton Conduction in Perovskite type oxide solid solution, Solid State Ionics, Rev. Chim. Miner. 17 (1980) 243-253.

[8] H .Iwahara, H .Uchida, K. Ono, K. Ogaki, Proton conduction in sintered oxides based on $BaCeO_3$, J Electro Chem Soc. 135 (1988) 529-33.

[9] M.M Amini,M. Mirzaee, Effect of solvent and temperature on the preparation of potassium niobate by hydrothermal-assisted sol–gel processing, Ceram Int .35 (2009) 2367–2372.

[10] Boschini F, Rulmont A, Cloots R, Vertruyen B Rapid synthesis of submicron crystalline barium zirconate BaZrO3 by precipitation in aqueous basic solution below 100°C,J EurCeram Soc. 29 (2009) 1457–1462.

[11] A.V.Orlov, O.A.Shlyakhtin,A, L.Vinokurov, A.V.Knotko,Yu.D.Tret Yakov, Preparation and properties of fine BaCeO3 powders for low temperature sintering, Inorganic Materials.Vol 41 11(2005)1194-1200.

[12] K.Katahira, Y. Kohchi, T.Shimura, H.Iwahara Protonic conduction in Zr-substituted $BaCeO_3$, Solid State Ion. 138 (2000) 91–98.

[13] K. Kinoshita, E.J. Cairns, "Fuel Cells "Encyclopedia of Chem. Technol. 11 (1994) 1098-1121.

[14] H. Iwahara, T.Yajima, H. Ushida, Effect of ionic radii of dopants on mixed ionic conduction (H^{++} O^{2-}) in $BaCeO_3$ based electrolytes.Solid State Ionics 70-71 (1994)

[15] J. Guan, S .E. Dorries, U. Balachandran, M. Liu, Transport properties of $BaCe_{0.95}Y_{0.05}O_{3-\delta}$ mixed conductors for hydrogen separation, Solid State Ionics. 100 (1997) 45-72.

[16] A. F. Sammells, R.L.Cook, J.H. White, J.J.Osborne, R.C.MacDuff, Solid State Ionics 52 (1992) 111.

[17] Zhen Shi, Et.al. Samarium and Yttrium Codoped BaCeO3 proton conductor with improved sinterability and higher Electrical Conductivity, Appl.Mater.Interfaces 6 (2014) 5175-5182.

[18] F. Deganello, G.Marci, G. Deganello. Citrate-nitrate auto combustion synthesis of perovskite-type nanopowders: a systematic approach, J Eur Ceram Soc. (2009) 29 439e50.

[19] R.R Chien, C.S Tu, V. Hugo-Schmidt, S.C Lee, Huang CC. Synthesis and characterization of proton-conducting $Ba(Zr_{0.8\_x}Ce_xY_{0.2})O_{2.9}$ ceramics, Solid State Ionics. (2010) 181 1251e7.

[20] F.Deganello, G.Marci, G.Deganello, Citrate-nitrate auto combustion synthesis of perovskite-type nanopowders: a systematic approach, J Eur Ceram Soc. (2009) 29 439e50.

[21] Ding H, Xue X, $BaZr_{0.1}Ce_{0.7}Y_{0.1}Yb_{0.1}O_{3\_\delta}$ electrolyte-based solid oxide fuel cells with cobalt-free $PrBaFe_2O_5$þd layered perovskite cathode, J Power Sources. 195 (2010) 7038e41.

[22] S.U.Dubai, A P.Jamale , C.H. Bhosale, L D.Jadhav, Proton conducting $BaCe_{0.7}Zr_{0.1}Y_{0.2}O_{2.9}$ thin films by spray deposition for solid oxide fuel cell, Applied Surface Science 324 (2015) 871-876.

[23] Yuji okuyama, Kaori Isa, Young Sung Lee, Takaai Sakai, Incorporation and conduction of proton in $SrCe_{0.9-x}Zr_xY_{0.1}O_{3-\delta}$, Solid State Ionics. 275 (2015) 35-38.

[24] H. Zheng, I.M. Reaney, G.D.C. Csete de Györgyfalva, R. Ubic, J. Yarwood, M.P. Seabra, VFerreira, Raman spectroscopy of $CaTiO_3$-based perovskite solid solutions, J. Mater. Res. 19 (2004) 488–495.

[25] HAOH, Study of A-site doping of $SrBi_4Ti_4O_{15}$ Bi-layered compounds using micro-Raman spectroscopy, Appl. Phys. A. 85 (2006) 69.

[26] A.S.Babu, Ranjit Bauri, Synthesis, phase stability and conduction behavior of rare earth and transition metals doped barium cerates, International journal of hydrogen energy. 39 (2014) 14487-14495.

[27] K. CS Ouzaouit, A. Benlhachemi, H. Benyaich, J. P. Dallas, S. Villain, J. A. Musso, J. R. Gavarri, Electrical conductivity of BaCeO3 synthesized by new sol-gel Method, *M*.J.Condensed Matter Physics.Vol7 (2006) 6.

[28] B. Surinderjt Singh, T.Fursenhaupt, R.Paul, T. Venkatraman, Synthesis, Structure-chemical stability and electrical properties of Nb-Zr and Nb codoped $BaCeO_3$ perovskites, Inorganic Chemistry.50 (2001) 6493-6499.

[29] R.Vasudevan , Synthesis And characterization of $BaCeYO_3$ and $BaZrYO_3$ composites for solid oxide fuel cell applications and microwave sintering of nanoceramics, shodhganga (2013) http://hdl.handle.net/10603/24545.

[30] V.M. Jali, S. Aparna, Ganesh Sanjeev, S.B. Krupanidhi, Ac conductivity studies on the electron irradiated BaZrO3 Ceramic, Nuclear Instruments and methods in physics research B. 257 (2007) 505-509.